





Cite this: *Phys. Chem. Chem. Phys.*,  
2019, 21, 6327

# Solving the Schrödinger equation of hydrogen molecules with the free-complement variational theory: essentially exact potential curves and vibrational levels of the ground and excited states of the $\Sigma$ symmetry†

Yusaku I. Kurokawa, \* Hiroyuki Nakashima  and Hiroshi Nakatsuji \*

The Schrödinger equation of hydrogen molecules was solved essentially exactly and systematically for calculating the potential energy curves of the electronic ground and excited states of the  $^1\Sigma_g$ ,  $^1\Sigma_u$ ,  $^3\Sigma_g$ , and  $^3\Sigma_u$  symmetries. The basic theory is the variational free complement theory, which is an exact general theory for solving the Schrödinger equation of atoms and molecules. The results are essentially exact with the absolute energies being correct beyond  $\mu$ -hartree digits. Furthermore, all of the present wave functions satisfy correct orthogonalities and Hamiltonian-orthogonalities to each other at every nuclear distance along the potential curve, which makes systematic analyses and discussions possible among all the calculated electronic states. It is noteworthy that these conditions were not satisfied in many of the accurate calculations of  $H_2$  reported so far. Based on the present essentially exact potential curves, we calculated and analyzed the vibrational energy levels associated with all the electronic states. Among them, the excited states having double-well potentials showed some interesting features of the vibrational states. These results are worthy of future investigations in astronomical studies.

Received 21st September 2018,  
Accepted 22nd October 2018

DOI: 10.1039/c8cp05949g

rsc.li/pccp

## 1. Introduction

Solving the Schrödinger equation (SE) is a paramount theme of quantum chemistry because it is a governing principle of chemical phenomena. A general exact theory for solving the SE was proposed by one of the authors.<sup>1–5</sup> It was initially called free ICI theory and later renamed as free complement (FC) theory. The FC theory produces the complement functions (cf's)  $\{\phi_i\}$  with which the exact solution of the SE is described as  $\psi = \sum C_i \phi_i$ : the FC wave function has a potentially exact structure so that after applying the variational principle, we can get the exact wave function. This FC-variation principle (VP) method<sup>3</sup> is straightforward and accurate when one can evaluate the matrix elements in the Hamiltonian and overlap matrices analytically, though such cases are limited only for some small systems. We have applied the FC-VP method to solve the SE of small systems, like helium atoms,<sup>6–8</sup> hydrogen molecular ions in the ground and excited states in both Born–Oppenheimer

(BO) and non-BO levels,<sup>9–12</sup> and hydrogen molecules at the equilibrium geometry in the ground state.<sup>13</sup> Their solutions were extremely accurate with satisfying the variational principle: the calculated absolute energies always keep upper bounds to the exact ones.

On the other hand, when analytical evaluations of the overlap and Hamiltonian matrices over the complement functions are difficult, we use the local SE's at many sampling points over the target atoms or molecules as the conditions to determine the coefficients of the complement functions. This method is called the local Schrödinger equation (LSE) method.<sup>4</sup> The LSE method is an integral-free method, so that one can apply it to any systems and any type of cf's. This method has been applied to various atoms and small organic and inorganic molecules and gave highly accurate energies satisfying chemical accuracy (less than 1 kcal mol<sup>-1</sup> as the absolute energy) for both the ground and excited states.<sup>5,14–17</sup>

In this study, we systematically investigate the electronic ground and excited states of the hydrogen molecule. We solve the BO SE of a hydrogen molecule in the ground and lower excited states almost exactly by the FC-VP theory: all the integrals involved are calculated analytically. We calculate highly accurate PECs of the  $^1\Sigma_g$ ,  $^1\Sigma_u$ ,  $^3\Sigma_g$ , and  $^3\Sigma_u$  symmetries.

Quantum Chemistry Research Institute, The Kyoto Technoscience Center 16,  
14 Yoshida Kawara-machi, Sakyo-Ku, Kyoto 606-8305, Japan.

E-mail: y.kurokawa@qcri.or.jp, h.nakatsuji@qcri.or.jp

† Electronic supplementary information (ESI) available. See DOI: 10.1039/c8cp05949g

The calculated wave functions at each nuclear distance  $R$  of state  $n$ ,  $\psi_n(R)$ , satisfy

$$\hat{H}(R)\psi_n(R) = E_n(R)\psi_n(R), \quad (1)$$

$$\langle \psi_n(R) | \psi_m(R) \rangle = \delta_{mn}, \quad (2)$$

and

$$\langle \psi_n(R) | \hat{H}(R) | \psi_m(R) \rangle = E_n(R)\delta_{mn}, \quad (3)$$

where  $E_n$  is the electronic energy of state  $n$ . Then, from these PECs, we systematically calculate almost all the vibrational energy levels associated with each electronic state.

The study of the accurate wave functions of hydrogen molecules has a long history since it is the simplest molecule and is very often used as the benchmark study for new quantum chemistry calculations. In 1933, as a pioneering study, James and Coolidge (JC)<sup>18</sup> succeeded in obtaining very accurate energies and the equilibrium geometries of the hydrogen molecule. Sims and Hagstrom improved the JC type wave function and obtained the PECs in the  $^1\Sigma_g$  symmetry.<sup>19</sup> In 1965, Kolos and Wolniewicz (KW) reported the wave functions<sup>20</sup> that cover the whole region of the internuclear distance  $R$  for the ground and several excited states. The KW type wave functions were applied to various states of different spin and spatial symmetries,<sup>21–29</sup> but their methods were state-specific so that their wave functions were not guaranteed to be orthogonal and Hamiltonian-orthogonal with those in the other states. In 1995, Cencek, Komasa, and Rychlewski showed that the explicitly correlated Gaussian (ECG) type wave functions give very accurate energies for the  $^3\Sigma_g$ ,  $^3\Sigma_u$ ,  $^1\Sigma_u$ ,  $^1\Pi_u$ , and  $^1\Sigma_g$  states.<sup>30</sup> Adamowicz *et al.* also performed non-adiabatic calculations using the ECG wave functions and very accurate vibrational levels for the ground state.<sup>31</sup> In 2009, Corongiu and Clementi employed the full CI method and calculated the PECs of the ground and 12 excited states in the  $^1\Sigma_g$  state.<sup>32,33</sup> Recently, in 2013, Pachucki reported very precise energies for the  $^1\Sigma_g$  states at some  $R$  values.<sup>34,35</sup> The accurate calculations of the triplet states:  $^3\Sigma_g$  and  $^3\Sigma_u$  symmetries were also reported by Hagstrom *et al.* and Pachucki and Komasa.<sup>36,37</sup> Also, the PECs of several states were reported by the experiments.<sup>38,39</sup>

In most of the above literature of the theoretical studies, several target states were selected and computed state-specifically. Therefore, the physical features among the states had not been discussed systematically. On the other hand, in the present study, all the calculated states satisfy orthogonality and Hamiltonian orthogonality to each other between the different states, which is a necessary condition for the exact solutions of the Schrödinger equation. This is so for all the distances along the potential energy curves, from which we systematically calculated the vibrational energy levels associated with each potential curve of a different state.

In the present FC calculations, we dealt with the  $\lambda$  functions with negative powers which were used originally in the previous study of hydrogen molecules with the FC theory.<sup>13</sup> This type of functions (defined in Section IIB) is very important for small  $R$  and near-equilibrium distance,<sup>13</sup> but these  $\lambda$  functions have not used in other literature studies.

Recently, we were also successful in calculating the highly accurate PECs of the ground and various excited states by the FC-LSE method, *i.e.* using a sampling method. With the FC-LSE method, the computations are much easier than the present analytical FC-VP method since no integrations are necessary there, though the variational principle is not always satisfied and special care about sampling dependency is required. The results of the FC-LSE calculations will be published elsewhere.<sup>40</sup>

## II. Free complement theory

The FC theory is a general theory of solving the Schrödinger equations, and the details of this theory were explained in previous studies.<sup>2,3,5</sup> We explain here only the points pertinent to the present study. The FC wave function of order  $n$  is represented as a linear combination of the complement functions (cf's)  $\{\phi^{(n)}\}$ , given by

$$\psi_n = \sum_{i=1}^{M^{(n)}} C_i^{(n)} \phi_i^{(n)}. \quad (4)$$

The coefficients  $\{C^{(n)}\}$  are determined by the variational principle, *i.e.*, by solving the secular equation,  $\mathbf{HC} = \mathbf{ESC}$ , where  $\mathbf{H}$  and  $\mathbf{S}$  are the Hamiltonian and overlap matrices, respectively. Each energy value is the upper bound to the exact energy according to the variational principle, and the wave function is always orthogonal to each other since both  $\mathbf{H}$  and  $\mathbf{S}$  are Hermite matrices. The  $\{\phi^{(n)}\}$  is generated from an initial function  $\psi_0$  by using the following simplest iterative complement (SIC) formula,

$$\psi_{n+1} = [1 + C_{ng}g(\hat{H} - E_n)]\psi_n, \quad (5)$$

where  $g$  is a scaling function that was introduced to overcome the singularity problem caused by the singular Coulomb potentials existing in the Hamiltonian of atoms and molecules.<sup>2,3,5</sup>  $C_n$  and  $E_n$  are the coefficient and energy at the iteration  $n$  in the SIC formula, respectively. We perform the operation of eqn (5)  $n$  times from  $\psi_0$  and select only linearly independent and non-divergent functions as  $\{\phi^{(n)}\}$  in the right-hand side of eqn (5). The number of the selected function is defined as dimension:  $M^{(n)}$ . The  $\psi_n$  determined by eqn (4) is guaranteed to converge to the exact solution of the SE as the order  $n$  increases.<sup>2,3,5</sup>

### A. Initial wave function

In the FC theory, we first need to select an appropriate initial wave function  $\psi_0$ . The converging speed to the exact solution depends on the choice of  $\psi_0$ . In our previous study of hydrogen molecules for the ground state,<sup>13</sup> we employed the JC type function as  $\psi_0$ . In the present study, we modified it and employed

$$\begin{aligned} \psi_0 = \hat{A} & \left[ \exp(-r_{1A} - r_{2B}) + \exp\left(-r_{1A} - \frac{1}{2}r_{2B}\right)(1 - r_{2B}) \right. \\ & \left. + \exp\left(-r_{1A} - \frac{1}{3}r_{2B}\right)(1 - r_{2B} + r_{2B}^2) \right], \end{aligned} \quad (6)$$

as our initial wave function, where  $r_{iX}$  represents the distance between electron  $i$  and nucleus X (X = A or B), and  $\hat{A}$  is the

symmetry-adaptation operator, which will be explained in Section IIC. The first, second, and third terms in the brackets in eqn (6) ensured that the wave function correctly dissociates to H(1s)–H(1s), H(1s)–H( $n = 2$ ), and H(1s)–H( $n = 3$ ) states, respectively. We fixed the orbital exponents (the coefficient of  $r_{iX}$  in the exp functions) as given in eqn (6) in the whole regions of the PECs. This has three merits: the first is that the resultant PECs dissociate into the correct states, the second is that the PECs are smooth because we do not do any non-linear optimizations at each  $R$ , and the third is that one can save the computational time. The demerit of the fixed exponents is that the descriptions of the wave function in the bonding region may become worse than those of the dissociated region. This demerit, however, can be overcome with the FC theory automatically by increasing its order.

## B. Hamiltonian and complement functions in elliptic coordinates

We employ the elliptic coordinates whose variables are defined as  $\lambda_i \equiv (r_{iA} + r_{iB})/R$ ,  $\mu_i \equiv (r_{iA} - r_{iB})/R$ , where  $R$  is the distance between the nuclei A and B, and  $\varphi_i$ , which is the azimuthal angle around the molecular axis ( $i = 1$  and  $2$ ). We further use supplementary variables,  $\rho$ , defined by  $\rho \equiv \frac{2}{R}r_{12}$ .

Using the elliptic coordinates, the initial wave function (6) is rewritten generally as

$$\psi_0 = \sum_i^{M^{(0)}} C_i \hat{A} \exp(-\alpha_{1i}\lambda_1 - \alpha_{2i}\lambda_2 - \beta_{1i}\mu_1 - \beta_{2i}\mu_2) \lambda_1^{m_i} \lambda_2^{n_i} \mu_1^{j_i} \mu_2^{k_i}. \quad (7)$$

The exponents  $\alpha$  and  $\beta$  in eqn (7) change as the inter-nuclear distance changes due to the existing  $R$  in  $\lambda$  and  $\mu$  coordinates.

The kinetic operator and the potential in the Hamiltonian are written as

$$\nabla_i^2 = \frac{4}{R^2(\lambda_i^2 - \mu_i^2)} \left[ \frac{\partial}{\partial \lambda_i} (\lambda_i^2 - 1) \frac{\partial}{\partial \lambda_i} + \frac{\partial}{\partial \mu_i} (1 - \mu_i^2) \frac{\partial}{\partial \mu_i} + \left( \frac{1}{\lambda_i^2 - 1} + \frac{1}{1 - \mu_i^2} \right) \frac{\partial^2}{\partial \varphi_i^2} \right] \quad (8)$$

and

$$\hat{V} = \frac{2}{R} \left[ -\frac{\lambda_1}{\lambda_1^2 - \mu_1^2} - \frac{\lambda_2}{\lambda_2^2 - \mu_2^2} + \frac{1}{\rho} + \frac{1}{2} \right], \quad (9)$$

respectively, in the elliptic coordinates. The  $g$  function employed in this study is

$$g = 1 + \frac{\lambda_1^2 - \mu_1^2}{\lambda_1} + \frac{\lambda_2^2 - \mu_2^2}{\lambda_2} + \rho, \quad (10)$$

where the second and third terms correspond to the inverse orders of the electron–nucleus potentials of electrons 1 and 2,  $1/r_{1A} + 1/r_{1B}$  and  $1/r_{2A} + 1/r_{2B}$ , respectively, and the fourth term corresponds to the inverse order of the electron–electron repulsive potential  $1/r_{12}$ . When we operate the kinetic and potential operators

and the  $g$  function on  $\psi_0$  according to eqn (5), we obtain the general expression of the cf's as

$$\phi_i = \hat{A} \exp(-\alpha_{1i}\lambda_1 - \alpha_{2i}\lambda_2 - \beta_{1i}\mu_1 - \beta_{2i}\mu_2) \lambda_1^{m_i} \lambda_2^{n_i} \mu_1^{j_i} \mu_2^{k_i} \rho^{p_i}. \quad (11)$$

Note that the integers  $j$ ,  $k$ , and  $p$  that appear as the power of  $\mu_1$ ,  $\mu_2$ , and  $\rho$ , respectively, take zero and positive and the integers  $m$  and  $n$  (the power of  $\lambda_1$  and  $\lambda_2$ , respectively) take negative, zero, and positive in the cf's. The cf's with the negative power of  $\lambda_1$  and/or  $\lambda_2$ , which have not been used in the other literature studies, are our original and first used in our study. Their efficiencies were examined in the previous study,<sup>13</sup> and they would be important to describe especially the bonding region.

## C. Symmetry adaptation

The symmetry adaptation operator,  $\hat{A}$ , in eqn (6) is defined as  $\hat{A} = \hat{P}_{\text{spin}} \hat{P}_{\text{space}}$ , where

$$\begin{aligned} \hat{P}_{\text{spin}} &\equiv 1 + \hat{P}_{12} \text{ (for singlet)} \\ &\equiv 1 - \hat{P}_{12} \text{ (for triplet)} \end{aligned} \quad (12)$$

$$\begin{aligned} \hat{P}_{\text{space}} &\equiv 1 + \hat{P}_{\text{AB}} \text{ (for gerade)} \\ &\equiv 1 - \hat{P}_{\text{AB}} \text{ (for ungerade)}, \end{aligned} \quad (13)$$

and  $\hat{P}_{12}$  interchanges the electrons 1 and 2 as  $\hat{P}_{12} = \{\lambda_1 \leftrightarrow \lambda_2, \mu_1 \leftrightarrow \mu_2\}$  and  $\hat{P}_{\text{AB}}$  interchanges the nuclei A and B as  $\hat{P}_{\text{AB}} = \{\mu_1 \leftrightarrow -\mu_1, \mu_2 \leftrightarrow -\mu_2\}$ . The combinatorial use of these operators can express the  $^1\Sigma_g$ ,  $^1\Sigma_u$ ,  $^3\Sigma_g$ , and  $^3\Sigma_u$  states from the common initial wave function.

## D. Integral evaluation

The Hamiltonian matrix  $\mathbf{H}$  and the overlap matrix  $\mathbf{S}$  of the cf's are defined by  $H_{ij} \equiv \langle \phi_i | \hat{H} | \phi_j \rangle$  and  $S_{ij} \equiv \langle \phi_i | \phi_j \rangle$ , respectively. The integrands are the linear combination of the following basic integrals:

$$I = \int \exp(-\alpha_1 \lambda_1 - \alpha_2 \lambda_2 - \beta_1 \mu_1 - \beta_2 \mu_2) \lambda_1^m \lambda_2^n \mu_1^j \mu_2^k \rho^p d\lambda_1 d\lambda_2 d\mu_1 d\mu_2 d\varphi_1 d\varphi_2 \quad (14)$$

where  $j$ ,  $k$ , and  $p$  take zero or positive integers,  $m$  and  $n$  take negative, zero, or positive integers, the integration ranges of each of the variables are,  $1 \leq \lambda_i \leq \infty$ ,  $-1 \leq \mu_i \leq 1$ , and  $0 \leq \varphi_i \leq 2\pi$  ( $i = 1, 2$ ), and the Jacobian  $J \equiv \frac{R^6}{64} (\lambda_1^2 - \mu_1^2) (\lambda_2^2 - \mu_2^2)$  is already considered and expanded in the integrands.

To evaluate eqn (14), the  $\rho^p$  is reduced to  $\rho^0$  when  $p$  is even or to  $\rho^{-1}$  when  $p$  is odd using the relation

$$\begin{aligned} \rho^2 &= \lambda_1^2 + \lambda_2^2 + \mu_1^2 + \mu_2^2 - 2\lambda_1 \lambda_2 \mu_1 \mu_2 \\ &- 2[(\lambda_1^2 - 1)(\lambda_2^2 - 1)(1 - \mu_1^2)(1 - \mu_2^2)]^{\frac{1}{2}} \cos(\varphi_1 - \varphi_2) \end{aligned} \quad (15)$$

repeatedly.

The  $\rho^{-1}$  can be expanded using the Neuman's expansion,

$$\rho^{-1} = \sum_{\tau=0}^{\infty} \sum_{N=0}^{\infty} D_{\tau}^N P_{\tau}^N \begin{pmatrix} \lambda_1 \\ \lambda_2 \end{pmatrix} Q_{\tau}^N \begin{pmatrix} \lambda_2 \\ \lambda_1 \end{pmatrix} P_{\tau}^N(\mu_1) P_{\tau}^N(\mu_2) \cos[N(\varphi_1 - \varphi_2)], \quad (16)$$

where  $D_{\tau}^0 = 2\tau + 1$ ,  $D_{\tau}^N = 2(2\tau + 1)[(\tau - N)!/(\tau + N)!]^2$  ( $N > 0$ ), and  $P$  and  $Q$  are the associated Legendre functions of the first and second kinds, respectively, and we take the upper variables when  $\lambda_2 \geq \lambda_1$  and the lower ones otherwise. Then, the integrand in eqn (14) is decomposed into a sum of products of  $\lambda_1$  and  $\lambda_2$  parts, the  $\mu_1$  part, the  $\mu_2$  part, and the  $\varphi_1$  and  $\varphi_2$  parts. We can integrate over these variables separately. In the  $\tau$  summation in eqn (16), we truncate it when the summed value reaches in more than 60-digit accuracy. In integrating the  $\lambda_2$  part, we need to evaluate the integral

$$I' = \int_{\lambda_2=1}^{\infty} \exp(-\alpha\lambda_2) E_i(-\beta\lambda_2) \lambda_2^m \ln\left(\frac{\lambda_2 + 1}{\lambda_2 - 1}\right) \quad (17)$$

and related ones. These integrations including the  $E_i$  functions with negative  $m$  were calculated numerically using the Maple program.<sup>41</sup> All the other calculations were done using the GMP (GNU multiple precision arithmetic) library.<sup>42</sup>

### III. Convergence of the FC wave function

In Table 1, the numbers of the cf's  $M^{(n)}$  generated at order  $n = 0, 1, 2,$  and  $3$  are presented for each symmetry,  $^1\Sigma_g$ ,  $^1\Sigma_u$ ,  $^3\Sigma_g$ , and  $^3\Sigma_u$ . A set of the cf's at order  $n$  always includes those at lower orders  $m$  ( $m < n$ ). At order  $n = 0$ , the number of the initial wave functions is  $M^{(0)} = 10$  for the  $^1\Sigma_g$  and  $^3\Sigma_u$  symmetries, but  $M^{(0)} = 9$  for the  $^1\Sigma_u$  and  $^3\Sigma_g$  symmetries. This is because the  $\exp(-r_{1A} - r_{2B})$  term in the initial wave function, which represents the H(1s)–H(1s) state at the dissociation limit, vanishes when the symmetry-adaptation operator is applied as explained in Section IID. For the same reason, the numbers of the generated cf's are different for each symmetry at order = 1, 2, and 3. All cf's at order  $n = 3$  in the  $^1\Sigma_g$ ,  $^1\Sigma_u$ ,  $^3\Sigma_g$ , and  $^3\Sigma_u$  states are listed in Tables S1–S4, respectively, in the ESI.†

We calculated the energies and the FC wave functions, changing the inter-nuclear distance  $R$  at order  $n = 0, 1, 2,$  and  $3$ . We call the lowest eigenvalue in each symmetry  $E_0$ , and second, third, . . . solutions  $E_1, E_2, \dots$ . We also use the Herzberg's notation for known states. To check the convergence of the FC wave functions, Fig. 1 shows the PECs of the  $^1\Sigma_g$  state at  $n = 0, 1, 2,$  and  $3$ , and their energies are shown in Table 2 at the selected inter-nuclear distances. As the order  $n$  increases, the

energies converge from the above to the exact values cited at the bottom of each distance in Table 2. It was observed that, at  $n = 2$ , the energies of each state have more than 3-digit accuracies at each distance, except for short inter-nuclear distances in the  $E_2$ (GK),  $E_3$ (HĤ),  $E_4$ (P) and  $E_5$ (O) states. At  $n = 3$ , the energies of each state almost converged to the exact values, and they have  $\mu$ -hartree accuracies or better, as discussed below. These observations hold true for the other symmetry states. In the following discussions, we use the current best results at  $n = 3$ , if not specially mentioned.

### IV. Potential energy curves

In Fig. 2, all the ground and excited PECs in the  $^1\Sigma_g$ ,  $^1\Sigma_u$ ,  $^3\Sigma_g$ , and  $^3\Sigma_u$  symmetries and vibrational levels associated with each PEC are shown. In Fig. 3–6, the PECs of the lowest six states of the  $\Sigma$  symmetry are separately plotted. The detailed energy values for each  $R$  are given in Tables S5–S8 of the ESI.† Note that the sixth states of the  $^1\Sigma_u$  and  $^3\Sigma_g$  symmetries, which dissociate to the H(1s)–H( $n = 4$ ) states, are not guaranteed to dissociate to the correct states in the present method because the proper wave functions for the H(1s)–H( $n = 4$ ) states are not included in the initial wave function. In the FC theory, however, the higher order of the cf's from other initial functions can accurately cover these states. We again emphasize that the present calculations are not state-specific: the ground and excited states are common eigenfunctions of the same Hamiltonian matrix of each symmetry,  $^1\Sigma_g$ ,  $^1\Sigma_u$ ,  $^3\Sigma_g$ , and  $^3\Sigma_u$ , at each  $R$ . This makes systematic discussions possible for all the calculated states and their PECs.

For the ground state of the  $^1\Sigma_g$  state, the total energy  $E_0(X)$  at the equilibrium geometry ( $R = 1.4011$  a.u.) is calculated to be  $E = -1.174475307$  a.u. as seen from Table 2. This has a  $\mu$ -hartree accuracy compared with the reference energy:  $E = -1.174475931400216$  a.u. from the 22 363-basis calculations by Pachucki.<sup>34</sup> The energies at  $R > 1.4$  a.u. also have  $\mu$ -hartree accuracies and those at  $R < 1.4$  a.u. have 5-digit accuracies, compared with those by Pachucki.<sup>34</sup>

The excited states of the  $^1\Sigma_g$  symmetry are also calculated accurately compared with the best values in the literature studies; the differences between the FC energies and the Pachucki's energies<sup>35</sup> are calculated to be  $\Delta E_0 = 1.98 \times 10^{-7}$  a.u.,  $\Delta E_1 = 3.30 \times 10^{-8}$  a.u.,  $\Delta E_2 = 1.43 \times 10^{-7}$  a.u.,  $\Delta E_3 = 1.90 \times 10^{-8}$  a.u.,  $\Delta E_4 = 4.90 \times 10^{-8}$  a.u., and  $\Delta E_5 = 7.96 \times 10^{-7}$  a.u. for the first (EF), second (GK), third (HĤ), fourth (P), and fifth (O) excited states, respectively, at  $R = 3.0$  a.u. At  $R = 6.0$  a.u., the energies are calculated to more than 7-digit accuracies. Similarly, the  $^1\Sigma_u$ ,<sup>28</sup>  $^3\Sigma_g$ ,<sup>27,36</sup> and  $^3\Sigma_u$ <sup>27,36,37</sup> states are calculated to more than 5-digit accuracy in the bonding regions ( $R = 2.0$  a.u.).

It was observed that the FC energy becomes more accurate with increasing  $R$ . For example, the FC energy has more than 10-digit accuracy at  $R = 10.0$  a.u. in the  $^1\Sigma_g$  state (the FC energy is  $E_0 = -1.000008755715$  a.u., and Pachucki gave  $E_0 = -1.000008755746$  a.u.),<sup>34</sup> while the FC energy has a  $\mu$ -hartree accuracy at the equilibrium geometry, as mentioned above.

Table 1 Number of the complement functions (cf's) at order  $n = 0, 1, 2,$  and  $3$  for different symmetries

State	Order			
	0	1	2	3
$^1\Sigma_g$	10	63	422	1819
$^1\Sigma_u$	9	58	386	1642
$^3\Sigma_g$	9	58	388	1609
$^3\Sigma_u$	10	63	424	1786

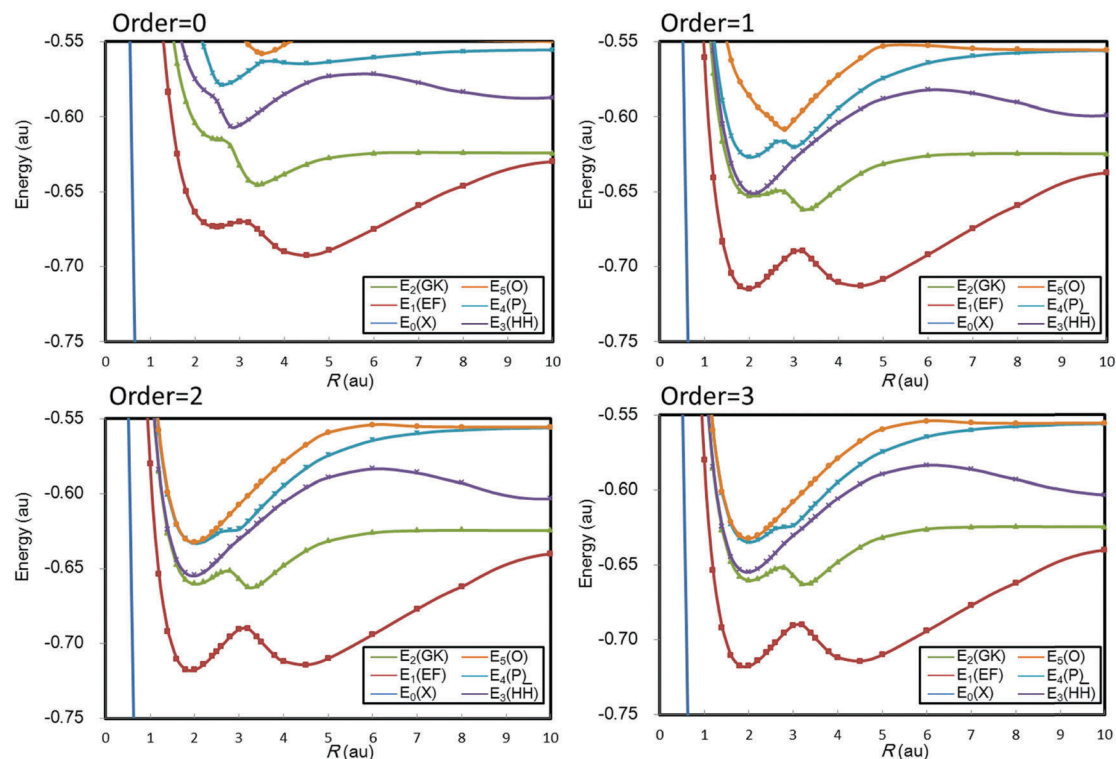


Fig. 1 Convergence of the FC energies at order  $n = 0, 1, 2,$  and  $3$  for the potential energy curves of hydrogen molecules in the  $1\Sigma_g$  state.

This observation applies also to the excited states. The reason why the FC energies become more accurate with increasing  $R$  is that the initial wave functions of the FC wave functions were chosen to be exact at the completely dissociated geometry, as explained in Section IIA.

At short inter-nuclear distances ( $R < 1.0$  a.u.), where the potential curve is repulsive and steep, the energies are less accurate; for example, the energy of the  $E_4$  state in the  $1\Sigma_u$  symmetry at  $R = 1.0$  a.u. has a milli-hartree accuracy.<sup>28</sup> This is because we do not include an appropriate wave function as the initial function for short  $R$ . To study very short inter-nuclear regions, it may be better to include a function for a united atom, such as the Chemical Orbital proposed by Clementi and Corongiu.<sup>33</sup>

We also note that, at many points of the calculated PECs, our results gave better energies than ever reported values; for example, our FC theory gave the energy  $E_5 = -0.632458510$  a.u. at  $R = 2.0$  a.u. of the  $1\Sigma_g$  state, while Wolniewicz and Dressler gave  $E_5 = -0.632457557$  a.u.<sup>25</sup> But at some points, our energies are a little worse than the reported values; for example, in the ground state of the  $1\Sigma_g$  symmetry, Pachucki gave better energies in the whole region.<sup>34</sup> However, it seems that our values have more than 5-digit accuracies in the bonding and dissociation regions of the PECs of the  $1\Sigma_g$ <sup>34</sup> and  $1\Sigma_u$ ,<sup>28</sup>  $3\Sigma_g$ ,<sup>27,36</sup> and  $3\Sigma_u$ <sup>27,36,37</sup> states. However, note that we have used less than 2000 functions to describe simultaneously the ground and excited states of each symmetry (see Table 1), whereas Wolniewicz and Dressler used the different basis function sets for different states since their calculations were state-specific.

It is known that the potential energy curves of some excited states have van der Waals minima at large nuclear distances:<sup>29</sup> Staszewska *et al.* gave the minima in the  $b^3\Sigma_u$  state (the ground state in the  $3\Sigma_u$  state) at  $R = 8.0$  a.u. with  $4.4369$   $\text{cm}^{-1}$  depth and in the  $e^3\Sigma_u$  state (the first excited state in the  $3\Sigma_u$  state) at  $R = 15.0$  a.u. with  $2.9993$   $\text{cm}^{-1}$  depth (the depth is the difference between the energy of the dissociation limit and the local minimum energy).<sup>27</sup> The present FC theory gives the minima for the  $b^3\Sigma_u$  state at  $R = 8.0$  a.u. with  $4.4380$   $\text{cm}^{-1}$  depth and in the  $e^3\Sigma_u$  state at  $R = 15.0$  a.u. with  $2.9998$   $\text{cm}^{-1}$  depth (see Table S8, ESI<sup>†</sup>). They gave another minimum in the  $h^3\Sigma_g$  state (the first excited state in the  $3\Sigma_g$  state) at  $R = 15.6$  a.u. with  $1.8338$   $\text{cm}^{-1}$  depth,<sup>27</sup> while the FC theory gives it at  $R = 15.6$  a.u. with  $1.8339$   $\text{cm}^{-1}$  depth (see Table S7, ESI<sup>†</sup>). Thus, the present method can describe such a small van der Waals interaction very accurately.

In Fig. 7, we also show the potential energy curves of the excited states higher than the sixth state for the  $1\Sigma_g$  symmetry, and their detailed values are listed in Table S9 (ESI<sup>†</sup>). Corongiu and Clementi already reported 12 excited states by the full CI method,<sup>32</sup> but we report here the 15 states by the FC-VP method. These energies are obtained as the higher eigenvalues of the secular equation and are the upper bounds to the exact values, but there are no initial functions corresponding to their dissociations. Nevertheless, these data would be still accurate and become useful references for the future theoretical and experimental studies.

Fig. 8 and Fig. S1 (ESI<sup>†</sup>) summarize all the PECs of the  $1\Sigma_g$ ,  $1\Sigma_u$ ,  $3\Sigma_g$ , and  $3\Sigma_u$  symmetries, calculated in this paper.

**Table 2** The energies (a.u.) of hydrogen molecules at the selected inter-nuclear distances in the  $^1\Sigma_g$  state calculated with the FC method at order  $n = 0, 1, 2$ , and  $3^a$ 

$R$ (a.u.)	Order	$E_0(X)$	$E_1(EF)$	$E_2(GK)$	$E_3(H\bar{H})$	$E_4(P)$	$E_5(O)$
0.5	0	-0.473160090	0.467150166	0.526489788	0.554210586	0.647965456	0.748789199
	1	-0.522270516	0.178662300	0.271787939	0.302046504	0.307437497	0.362205778
	2	-0.526517488	0.127170779	0.206447033	0.210128548	0.233044870	0.238357218
	3	-0.526636133	0.127042609	0.205960702	0.209276728	0.232336865	0.233707889
	Ref.	-0.526638758 <sup>b</sup>	0.127044530 <sup>c</sup>				
1.0	0	-1.097460370	-0.400906655	-0.340543336	-0.312559747	-0.219768603	-0.176895708
	1	-1.122793990	-0.560602662	-0.487470814	-0.467911114	-0.459860854	-0.401596139
	2	-1.124496291	-0.580068223	-0.508024388	-0.507783883	-0.483221875	-0.479786999
	3	-1.124538673	-0.580085427	-0.508066032	-0.507859752	-0.483310834	-0.483260350
	Ref.	-1.124539720 <sup>b</sup>	-0.580085101 <sup>c</sup>	-0.508065352 <sup>d</sup>	-0.507857287 <sup>d</sup>	-0.483309219 <sup>d</sup>	-0.483247664 <sup>d</sup>
1.4011	0	-1.151637266	-0.583738232	-0.523262560	-0.495015865	-0.409139152	-0.387201495
	1	-1.173265053	-0.683500301	-0.616199031	-0.604979087	-0.589610053	-0.536101526
	2	-1.174450788	-0.692155449	-0.626657136	-0.624549899	-0.600828388	-0.599117068
	3	-1.174475307	-0.692162609	-0.626679488	-0.624559939	-0.601824405	-0.600880012
	Ref.	-1.174475931 <sup>b</sup>					
2.0	0	-1.119487252	-0.663841484	-0.604125928	-0.575030024	-0.531480597	-0.464243660
	1	-1.137224888	-0.714988763	-0.652681227	-0.650634303	-0.626984693	-0.586189922
	2	-1.138116836	-0.717711177	-0.660423055	-0.654923977	-0.633261515	-0.632402335
	3	-1.138132582	-0.717715211	-0.660430062	-0.654926430	-0.634909096	-0.632458511
	Ref.	-1.138132957 <sup>b</sup>	-0.717714276 <sup>d</sup>	-0.660428175 <sup>d</sup>	-0.654926063 <sup>d</sup>	-0.634885512 <sup>d</sup>	-0.632457557 <sup>d</sup>
3.0	0	-1.047489133	-0.670000092	-0.632345999	-0.605622343	-0.573958494	-0.544594688
	1	-1.056767266	-0.690228452	-0.656010205	-0.628286094	-0.620220068	-0.602579339
	2	-1.057316865	-0.690744333	-0.656978883	-0.630548949	-0.623906192	-0.607306364
	3	-1.057326071	-0.690747023	-0.656985802	-0.630554115	-0.623922686	-0.607983717
	Ref.	-1.057326269 <sup>b</sup>	-0.690747056 <sup>e</sup>	-0.656985945 <sup>e</sup>	-0.630554134 <sup>e</sup>	-0.623922735 <sup>e</sup>	-0.607984513 <sup>e</sup>
6.0	0	-1.000100834	-0.659400228	-0.623820422	-0.577252084	-0.558001450	-0.547795548
	1	-1.000815298	-0.692111313	-0.625995288	-0.582171944	-0.564240910	-0.552563424
	2	-1.000835357	-0.694242391	-0.626146298	-0.583447929	-0.564423020	-0.553887236
	3	-1.000835702	-0.694266430	-0.626147956	-0.583463397	-0.564424570	-0.553905248
	Ref.	-1.000835708 <sup>b</sup>	-0.694267029 <sup>d</sup>	-0.626147969 <sup>d</sup>	-0.583463574 <sup>d</sup>	-0.564424574 <sup>d</sup>	-0.553905272 <sup>d</sup>
10.0	0	-1.000000522	-0.629934919	-0.624203739	-0.587207122	-0.555495453	-0.549842549
	1	-1.000008459	-0.637305568	-0.624627378	-0.599068694	-0.555923767	-0.555457695
	2	-1.000008753	-0.640213070	-0.624640969	-0.603362241	-0.555999881	-0.555538697
	3	-1.000008756	-0.640253722	-0.624641133	-0.603416613	-0.556000843	-0.555539183
	Ref.	-1.000008756 <sup>b</sup>	-0.640246025 <sup>d</sup>	-0.624641106 <sup>d</sup>	-0.603407271 <sup>d</sup>	-0.556000540 <sup>d</sup>	-0.555538599 <sup>d</sup>

<sup>a</sup> The complete data at order  $n = 3$  for the  $^1\Sigma_g$ ,  $^1\Sigma_u$ ,  $^3\Sigma_g$ , and  $^3\Sigma_u$  symmetries are listed in Tables S5–S8 in the ESI. <sup>b</sup> Ref. 34. <sup>c</sup> Ref. 26. <sup>d</sup> Ref. 25. <sup>e</sup> Ref. 35.

The lowest-energy curves of  $^1\Sigma_g$  and  $^3\Sigma_u$  dissociate to  $H(1s) + H(1s)$ , but there are no such dissociation channels in  $^1\Sigma_u$  and  $^3\Sigma_g$ . This is trivially understandable from their spatial and spin symmetries. By comparing the PECs of  $^1\Sigma_g$  and  $^1\Sigma_u$  with those of  $^3\Sigma_g$  and  $^3\Sigma_u$ , the former includes more complicated curves. This is due to the existence of the ionic channels that dissociates to  $H^- + H^+$  in  $^1\Sigma_g$  and  $^1\Sigma_u$ . On the other hand, no ionic channels exist in  $^3\Sigma_g$  and  $^3\Sigma_u$  where two electrons cannot occupy the same position in  $H^-$  due to the Pauli repulsion. At the dissociation limits of  $^1\Sigma_g$  and  $^1\Sigma_u$ , the energy of the ionic state:  $H^- + H^+$  is higher than that of  $H(1s) + H(n = 3)$ . However, since the ionic contribution indicates a long-range interaction proportional to  $1/R$ , the ionic curve moves from lower states to higher states, step by step, as approaching dissociation. Thus, the existence of the ionic term makes the PECs complicated and causes double-well potential shapes and state repulsions. Although the ionic channels indicate long-range behavior, the PECs showing that the ionic characters are dominant almost overlap between  $^1\Sigma_g$

and  $^1\Sigma_u$  at large  $R$ , for example, compare the EF state of  $^1\Sigma_g$  with the B state of  $^1\Sigma_u$ . This indicates that the origin of the long-range behavior is mainly explained from the classical ionic Coulombic interactions. In the present calculations, we do not explicitly employ the ionic terms, such as  $\exp(-r_{1A} - r_{2A})$ , into our initial functions. Nevertheless, all the PECs including ionic contribution can be accurately described at least near equilibrium distances. This is a numerical proof that the FC wave function converges to the exact solutions with increasing the FC order from any initial functions at the same symmetry. Actually, the cf's including  $\lambda^m$  terms, where  $m$  runs positive and negative integers, are two-centered functions and contain the ionic characters also with the covalent characters. However, explicitly introducing ionic-type functions into the initial function, the excited states containing ionic characters can be more efficiently described, especially for near the dissociations and/or higher excited states. In the forthcoming paper<sup>40</sup> by the FC-LSE method, we employ such ionic terms explicitly as the initial function and will do further discussions for their states.

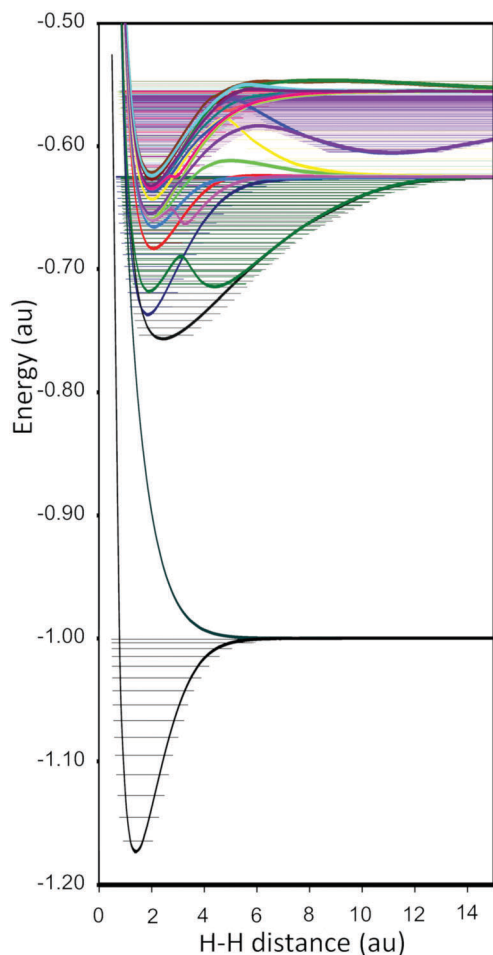


Fig. 2 All ground and excited potential energy curves (PECs) and vibrational levels associated with each PEC.

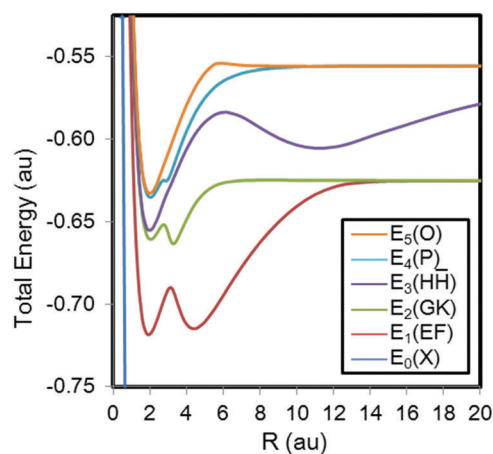


Fig. 3 The  $^1\Sigma_g$  potential energy curves of hydrogen molecules calculated by the FC method at order  $n = 3$ .

## V. Vibrational energy levels

Thus, we could evaluate very accurate PECs for the ground and excited states of  $\Sigma$  symmetries by the FC-VP method. Since their

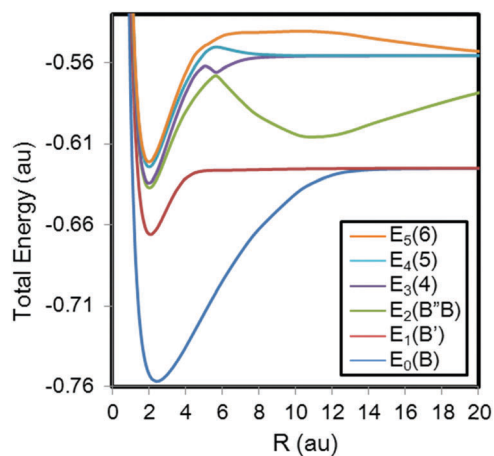


Fig. 4 The  $^1\Sigma_u$  potential energy curves of hydrogen molecules calculated by the FC method at order  $n = 3$ .

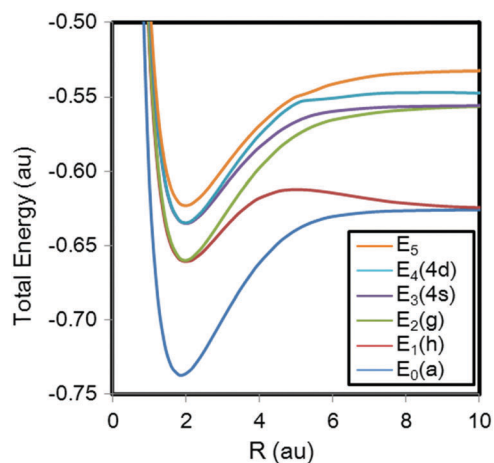


Fig. 5 The  $^3\Sigma_g$  potential energy curves of hydrogen molecules calculated by the FC method at order  $n = 3$ .

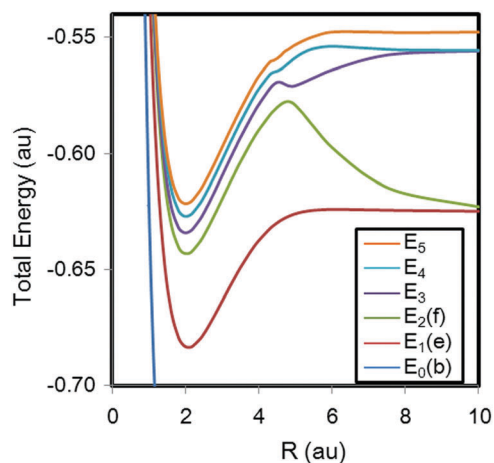


Fig. 6 The  $^3\Sigma_u$  potential energy curves of hydrogen molecules calculated by the FC method at order  $n = 3$ .

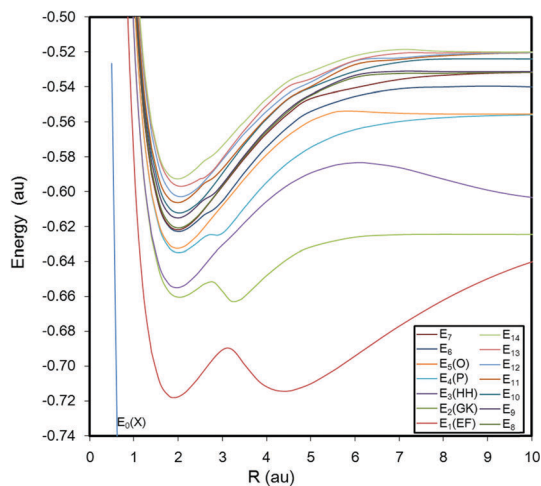


Fig. 7 The  $1\Sigma_g$  potential energy curves in the higher excited states of hydrogen molecules calculated by the FC method at order  $n = 3$ .

PECs are essentially exact, it is valuable to proceed to the vibrational analysis based on their accurate PECs. Here, we numerically solve the vibrational Schrödinger equations, given by

$$\left[ -\frac{1}{2\mu} \frac{d^2}{dR^2} + E_n(R) \right] \varphi_{v,n}(R) = V_{v,n} \varphi_{v,n}(R), \quad (18)$$

where  $E_n(R)$  is a potential energy function obtained by fitting the discrete PEC of state  $n$  with appropriate fitting functions,  $\mu$  is the reduced mass, and  $\varphi_{v,n}(R)$  and  $V_{v,n}$  are the vibrational wave function and the corresponding energy of the  $v$ -th state, respectively. For solving eqn (18), we actually used the Level 8 package by Le Roy.<sup>43</sup> Since the number of the points of  $R$  that we calculated at  $n = 3$  is limited, the highly accurate discrete PECs were interpolated and extrapolated and then obtained  $E_n(R)$ : for the interpolation, the cubic spline method was employed, and for the extrapolation of the outer region of the PECs, the energy values were fitted to the function  $E(R) = E_\infty - A/R^B$ , and for the extrapolation of the inner region of the PECs, the energy values were fitted to the function  $E(R) = E_0 + A \exp(-BR)$ .<sup>43</sup> Then, the vibrational SEs for each PEC in the  $1\Sigma_g$ ,  $1\Sigma_u$ ,  $3\Sigma_g$ , and  $3\Sigma_u$  symmetries were solved numerically, and the vibrational energy levels  $E_v$ , the expectation value of the nuclear distances  $\langle R \rangle$ , and those of the squared values  $\langle R^2 \rangle$  were obtained associated with all the calculated potential energy curves.

In Fig. 9, the calculated vibrational levels associated with the PECs of the ground and excited states are plotted. The vibrational levels in the sixth states of the  $1\Sigma_u$  and  $3\Sigma_g$  symmetries, which dissociate to the  $H(1s)-H(n=4)$  states, are not calculated since the PECs do not dissociate correctly, as explained in Section IV. The complete data for all the calculated vibrational levels are listed in Tables S10–S13 in the ESI,<sup>†</sup> where we listed only the lowest 50 vibrational states for the  $E_3(H\bar{H})$   $1\Sigma_g$  and  $E_2(B''\bar{B})$   $1\Sigma_u$  states because very high energy states would be highly dependent on the fitting method and may be unphysical. The ground state of the  $3\Sigma_u$  curve has no vibrational state because it is a repulsive curve. The three, six, one, and one highest vibrational levels for

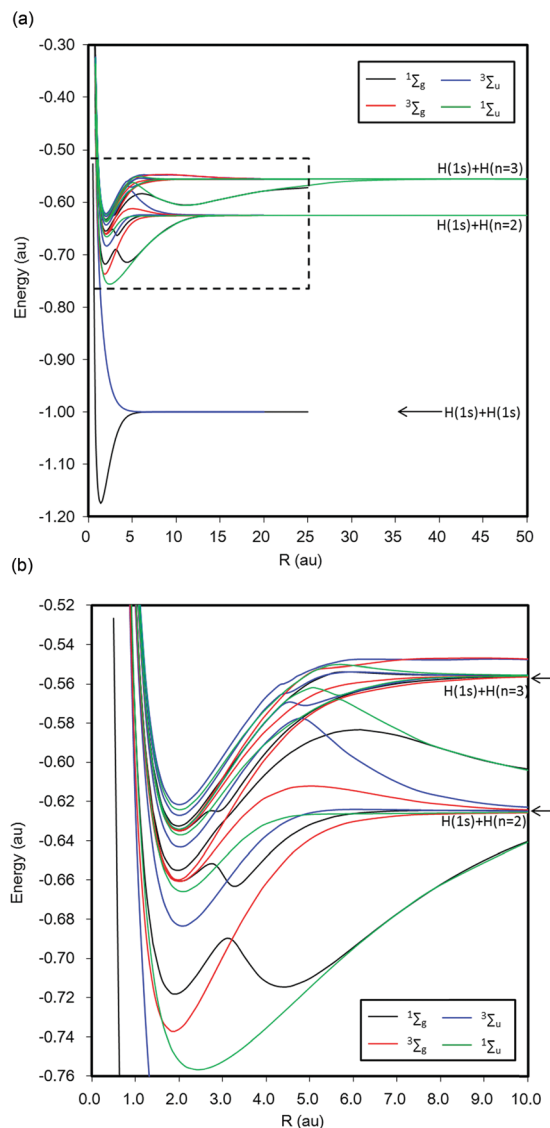


Fig. 8 (a) Potential curves of all the  $\Sigma$  states calculated by the FC method at order  $n = 3$ . The black, blue, red, and green curves are for the  $1\Sigma_g$ ,  $3\Sigma_u$ ,  $3\Sigma_g$ , and  $1\Sigma_u$  symmetries, respectively. The region in the broken line is enlarged in (b). (b) Enlarged figure of (a). Potential curves of all the  $\Sigma$  states calculated by the FC method at order  $n = 3$ . The black, blue, red, and green curves are for the  $1\Sigma_g$ ,  $3\Sigma_u$ ,  $3\Sigma_g$ , and  $1\Sigma_u$  symmetries, respectively.

the  $E_1(h)$   $3\Sigma_g$ ,  $E_2(f)$   $3\Sigma_u$ ,  $E_4(5)$   $1\Sigma_u$ , and  $E_5(O)$   $1\Sigma_g$  curves, respectively, are unstable because the outer region of these curves are repulsive and these vibrational levels are higher than the dissociation limit of their curves in energy. Fig. 10–13 are the calculated vibrational levels associated with the  $1\Sigma_g$ ,  $1\Sigma_u$ ,  $3\Sigma_g$ , and  $3\Sigma_u$  PECs, respectively. It is observed that, in the  $1\Sigma_g$  and  $1\Sigma_u$  states, the densities of the vibrational levels are sparse between  $E = -0.625$  and  $-0.604$  a.u. This is due to the very broad wells of the  $E_3(H\bar{H})$   $1\Sigma_g$  and  $E_2(B''\bar{B})$   $1\Sigma_u$  curves.

Table 3 summarizes some selected vibrational energy levels of the ground (X) and three excited states (EF, GK, and HH) in the  $1\Sigma_g$  symmetry and the  $\langle R \rangle$  and  $\langle R^2 \rangle$  values, the expectation value of the nuclear distance. We compared the vibrational

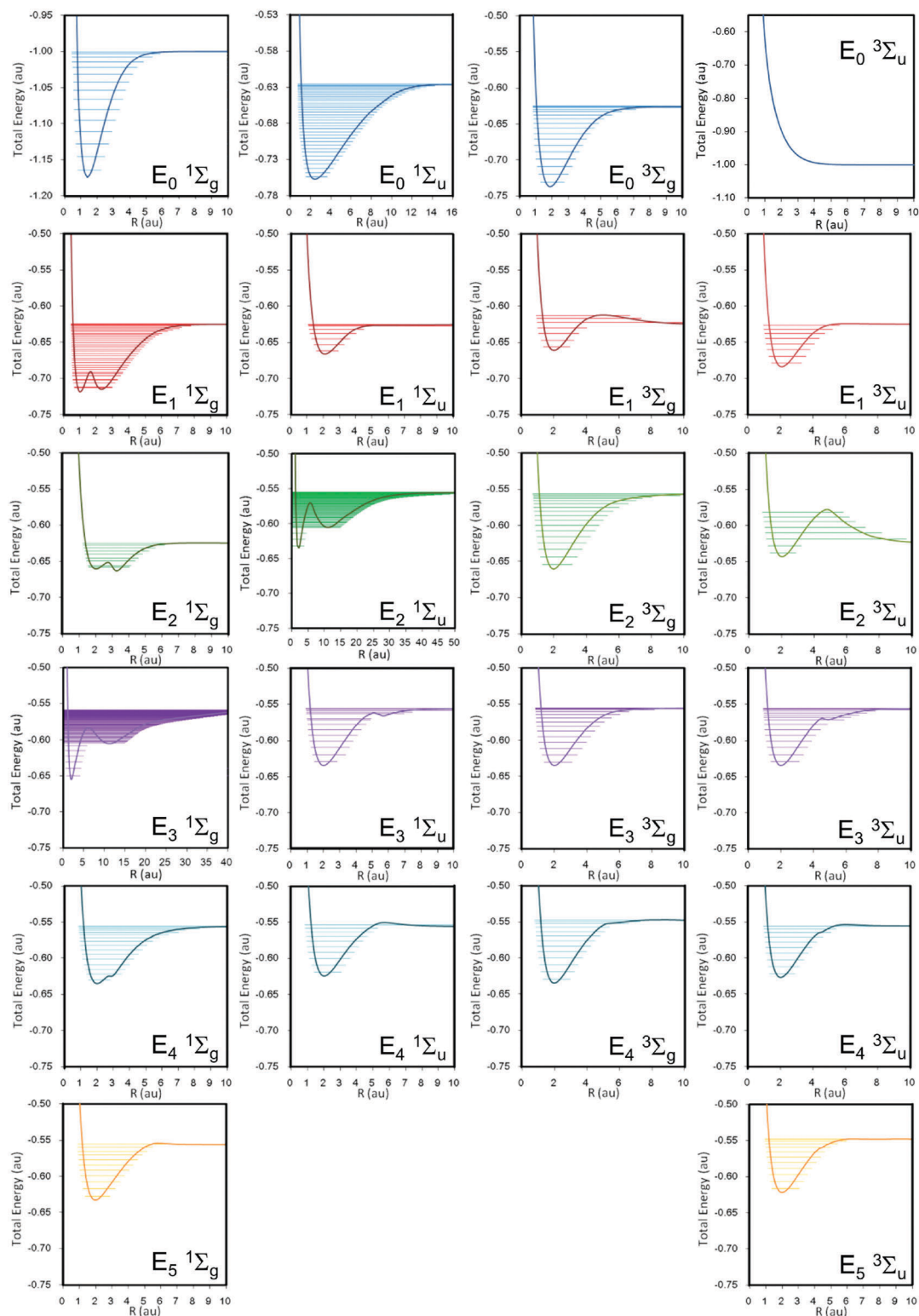


Fig. 9 All vibrational energy levels associated with each PEC calculated by the FC method at order  $n = 3$ . The numerical data are listed in Tables S10–S13 of the ESI.†

energy splitting:  $\Delta E_v (= E_v - E_{v-1})$  by the present method with those by theoretical and experimental references.<sup>22,31,39,45</sup> For simple single-well PECs, such as the ground state (X) of  $1\Sigma_g$ , and B state of  $1\Sigma_u$ , the present results agreed well with those by

the experiment in 2- or 3-digits. In these curves, as the vibrational level increases, the  $\langle R \rangle$  and  $\langle R^2 \rangle$  values gradually increase and the  $\Delta E_v$  value gradually decreases, which shows the anharmonicity of the potential. For the double-well PECs, such as the EF, GK,

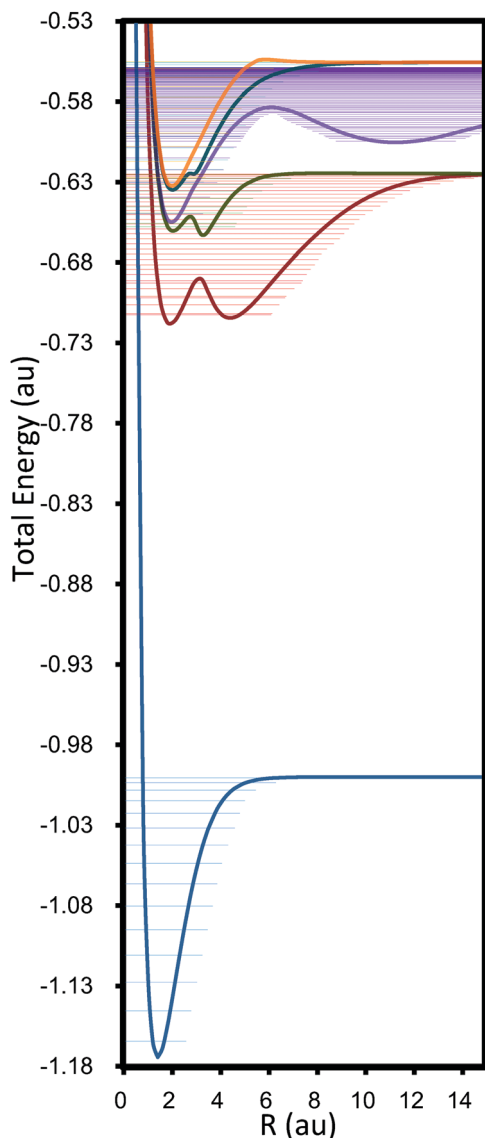


Fig. 10 All vibrational energy levels associated with the  ${}^1\Sigma_g$  PECs. The detailed energy values are given in Table S10 of the ESI.†

and  $\text{H}\ddot{\text{H}}$  states of  ${}^1\Sigma_g$ , our results only agreed with those of the experiment within 1- or 2-digits. This would be because non-adiabatic effects become important. Wolniewicz and Dressler<sup>25</sup> considered the non-adiabatic effects for some states and their correspondence with the experiments are improved. We do not consider their effects in the present study since the present purpose is to compute the vibrational energy levels systematically for all the calculated ground and excited states at the nonrelativistic (essentially exact) limits within the BO approximation.

Here, we especially focus on the discussions about the double-well PECs of the EF, GK, and  $\text{H}\ddot{\text{H}}$  states of the  ${}^1\Sigma_g$  symmetry since these states indicate interesting features due to the ionic contribution. The presence of a double minimum in these excited states was first theoretically demonstrated by Davidson.<sup>44</sup> Table 4 summarizes the positions  $R$  of the left- and right-local minima and the hill of the double wells of the

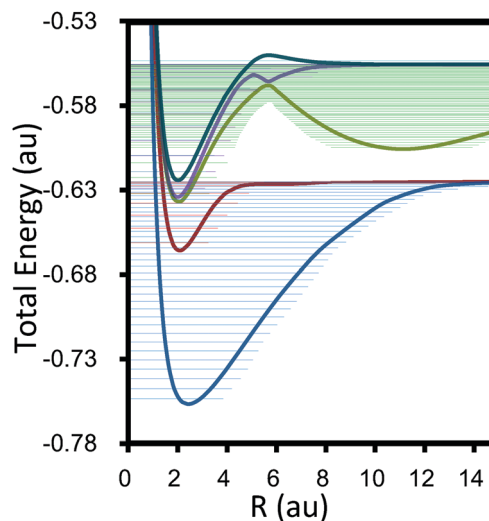


Fig. 11 All vibrational energy levels associated with the  ${}^1\Sigma_u$  PECs. The detailed energy values are given in Table S11 of the ESI.†

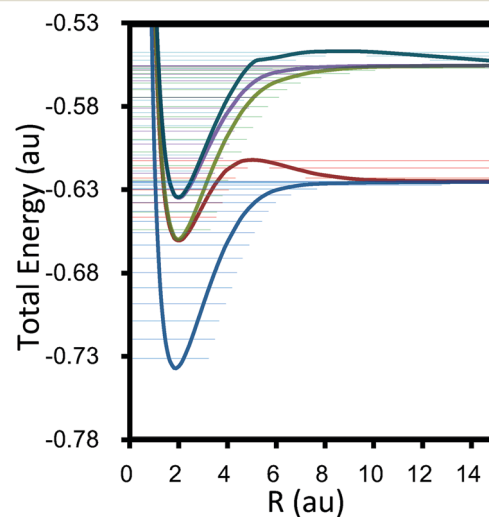


Fig. 12 All vibrational energy levels associated with the  ${}^3\Sigma_g$  PECs. The detailed energy values are given in Table S12 of the ESI.†

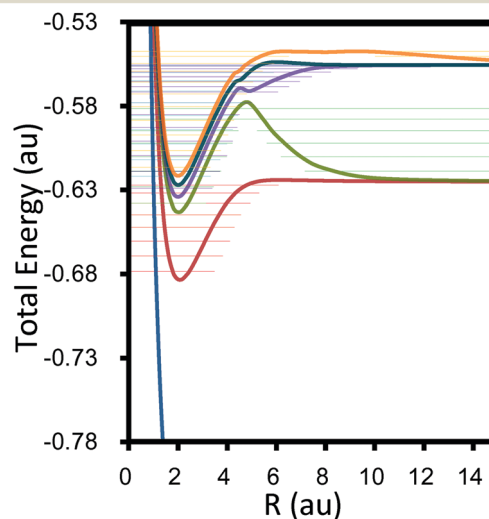


Fig. 13 All vibrational energy levels associated with the  ${}^3\Sigma_u$  PECs. The detailed energy values are given in Table S13 of the ESI.†

**Table 3** Vibrational energy levels  $E_v$  ( $\text{cm}^{-1}$ ) of the ground (X) and three low-lying excited states (EF, GK, and H $\bar{\text{H}}$ ) of  $^1\Sigma_g$ , calculated from the PECs of the FC method at order  $n = 3$  and the comparisons with other studies<sup>a</sup>

State	$\nu$	Assignment <sup>b</sup>	FC method				Ref. (theoretical)	Ref. (experimental)
			$\langle R \rangle^c$	$\langle R^2 \rangle^c$	$E_v^d$	$E_v - E_{v-1}$	$E_v - E_{v-1}$	$E_v - E_{v-1}$
X $^1\Sigma_g$	0		0.76646	0.59534	-255590.81		Stanke <i>et al.</i> <sup>e</sup>	Pardo <sup>f</sup>
	1		0.81797	0.69308	-251422.77	4168.03	4161.19	4161.14
	2		0.87099	0.79990	-247491.76	3931.02	3925.86	3925.79
	3		0.92594	0.91722	-243799.75	3692.01	3695.41	3695.43
	4		0.98420	1.04843	-240340.90	3458.84	3467.99	3467.95
	5		1.04705	1.19745	-237108.37	3232.53	3241.58	3241.61
	6		1.11551	1.36852	-234100.24	3008.13	3013.86	3013.86
	7		1.19085	1.56737	-231320.39	2779.85	2782.15	2782.13
	8		1.27536	1.80350	-228777.18	2543.21	2543.19	2543.25
	9		1.37269	2.09225	-226482.67	2294.51	2292.96	2292.93
	10		1.48885	2.45993	-224453.96	2028.71	2026.36	2026.38
EF $^1\Sigma_g$	0	Left	1.04654	1.10931	-156380.80		Wolniewicz <i>et al.</i> <sup>g</sup>	Bailly <i>et al.</i> <sup>h</sup>
	1	Right	2.35303	5.56457	-156203.48	177.32	198.73	199.10
	2	Right	2.41294	5.90780	-155009.06	1194.42	1195.67	1194.96
	3	Left	1.12820	1.32172	-154053.51	955.55	936.93	935.89
	4	Right	2.46532	6.23244	-153871.06	182.45	204.61	204.21
	5	Right	2.50233	6.49463	-152799.62	1071.43	1081.44	1079.28
	6	Left	1.51400	2.67541	-152027.49	772.13	783.97	781.37
	7	Right	2.30528	5.89949	-151725.39	302.10	285.74	278.97
	8		2.40554	6.35675	-150866.64	858.75	897.08	892.03
	9		2.12272	5.30197	-150192.15	674.49	671.55	654.32
	10		2.32806	6.30229	-149571.13	621.02	583.17	581.24
	11		2.48828	7.09208	-148837.58	733.55	749.94	746.89
	12		2.51076	7.31799	-148114.76	722.82	725.33	712.80
	13		2.57944	7.76638	-147417.63	697.12	681.99	672.64
	14		2.69065	8.41895	-146718.82	698.82	694.55	695.03
15		2.78398	9.00918	-146021.78	697.04	701.09	700.35	
GK $^1\Sigma_g$	0	Right	1.717483	2.98119	-144365.95		Wolniewicz <i>et al.</i> <sup>g</sup>	Bailly <i>et al.</i> <sup>h</sup>
	1	Left	1.163475	1.400071	-143909.19	456.76	360.60	183.82
	2		1.588394	2.652501	-142527.50	1381.69	1452.23	1580.81
	3		1.506582	2.476543	-141689.39	838.11	764.63	651.13
	4		1.707744	3.165721	-140546.42	1142.96	1145.83	1055.26
	5		1.775294	3.482897	-139520.59	1025.84	1001.21	1064.81
	6		1.971575	4.292311	-138589.65	930.94	892.81	916.76
	7		2.237863	5.509267	-137794.47	795.17	775.20	
8		2.757091	8.250715	-137235.43	559.04	523.71		
H $\bar{\text{H}}$ $^1\Sigma_g$	0	Left	1.077938	1.176718	-142576.61		Wolniewicz <i>et al.</i> <sup>g</sup>	Bailly <i>et al.</i> <sup>h</sup>
	1	Left	1.155198	1.380249	-140358.93	2217.68	2248.49	2293.94
	2	Left	1.253108	1.651700	-138350.21	2008.72	2130.59	2045.57
	3	Left	1.362133	1.975955	-136601.32	1748.89	1817.18	
	4	Left	1.444969	2.250600	-134989.12	1612.20	1476.75	
	5	Left	1.545178	2.594699	-133467.32	1521.79	1556.35	
	6	Right	5.949931	35.496886	-132669.76	797.56	694.39	
	7	Right	5.980785	36.060560	-132318.58	351.18	351.03	
	8	Left	1.653023	2.990029	-132071.04	247.54	308.81	
	9	Right	6.020838	36.747809	-131977.19	93.85	32.60	
	10	Right	6.069392	37.552327	-131646.03	331.16	331.93	
	11	Right	6.120844	38.407051	-131324.35	321.68	322.63	
	12	Right	6.175278	39.313906	-131011.38	312.97	313.51	
	13	Left	1.781358	3.486536	-130804.85	206.52	262.16	
	14	Right	6.233125	40.280642	-130706.79	98.06	42.45	
	15	Right	6.294557	41.312137	-130410.71	296.08	295.83	
	16	Right	6.359092	42.404713	-130123.20	287.50	287.20	
	17	Right	6.425669	43.546667	-129844.33	278.88	278.75	
	18	Left	1.935205	4.123028	-129682.18	162.15	218.56	
	19	Right	6.491295	44.701125	-129573.90	108.27	51.81	
	20	Right	6.553864	45.843374	-129311.76	262.14	262.10	
	21	Right	6.610493	46.940327	-129057.95	253.81	253.75	
	22	Right	6.653100	47.902398	-128812.82	245.13	245.14	
	23	Left	2.154131	5.135558	-128728.19	84.63	128.31	
	24	Right	6.680300	48.707079	-128576.71	151.48	107.92	
	25	Right	6.649869	48.873334	-128351.63	225.08	225.51	
26	Right	6.214292	44.670160	-128145.68	205.95	208.62		

Table 3 (continued)

State	$\nu$	Assignment <sup>b</sup>	FC method			Ref. (theoretical)	Ref. (experimental)
			$\langle R \rangle^c$	$\langle R^2 \rangle^c$	$E_V^d$	$E_V - E_{V-1}$	$E_V - E_{V-1}$
	27		4.060663	22.960315	-128020.74	124.95	141.54
	28		5.996018	43.795645	-127898.80	121.93	110.60
	29		6.312263	47.414667	-127718.73	180.07	176.89
	30		6.213519	46.940387	-127545.00	173.73	174.94

<sup>a</sup> The complete data for all the calculated vibrational levels associated with all the PECs of the ground and excited states of the  $^1\Sigma_g$ ,  $^1\Sigma_u$ ,  $^3\Sigma_g$ , and  $^3\Sigma_u$  symmetries are listed in Tables S10–S13 of the ESI. <sup>b</sup> Assignments of the vibrational states for the double-well potentials. <sup>c</sup> The expectation value of the nuclear distance  $R$  in Å and that of the squared value. <sup>d</sup> Absolute energies in  $\text{cm}^{-1}$ . <sup>e</sup> Ref. 31. <sup>f</sup> Ref. 39. <sup>g</sup> Ref. 22. <sup>h</sup> Ref. 45.

**Table 4** The positions of the minima (left and right) and the hill of the double wells of EF, GK, and H $\bar{H}$  states of  $^1\Sigma_g$  and the energy barriers:  $\Delta E_{\text{Left}} = E_{\text{Hill}} - E_{\text{Left}}$  and  $\Delta E_{\text{Right}} = E_{\text{Hill}} - E_{\text{Right}}$  from the left and right minima are summarized. The number of vibrational states lower than the hill is also summarized

$^1\Sigma_g$	$R_{\text{min(left)}} (\text{Å})$	$R_{\text{max(hill)}} (\text{Å})$	$R_{\text{min(right)}} (\text{Å})$	$\Delta E_{\text{Left}}: E_{\text{Hill}} - E_{\text{Left}} (\text{cm}^{-1})$	$\Delta E_{\text{Right}}: E_{\text{Hill}} - E_{\text{Right}} (\text{cm}^{-1})$	No. of vibrational states lower than the hill
EF	1.016	1.646	2.330	6290.14	5572.46	8
GK	1.080	1.446	1.736	1977.47	2519.57	2
H $\bar{H}$	1.050	3.211	6.152	15391.76	5682.20	27

EF, GK, and H $\bar{H}$  states of  $^1\Sigma_g$ . The energy barriers:  $\Delta E_{\text{Left}} = E_{\text{Hill}} - E_{\text{Left}}$  and  $\Delta E_{\text{Right}} = E_{\text{Hill}} - E_{\text{Right}}$  from the left- and right-local minima and the numbers of the vibrational states lower than the hill are also given in the table, which were 8, 2, and 27 for the EF, GK, and H $\bar{H}$  states, respectively. The assignments of these vibrational states are also given in Table 3. Fig. 14 illustrates the energy positions of the vibrational levels associated with the states: (a) EF, (b) GK, and (c) H $\bar{H}$ , respectively, on their PECs.

For the EF state, the left- and right wells are similar to each other, but the right well is a little bit broad. The numbers of states assigned to the left well were 4 and 5 to the right. The left and right minima locate at  $R = 1.016$  and  $2.330$  Å, respectively, and the position of the hill was  $1.646$  Å with the barriers:  $\Delta E_{\text{Left}} = 6290.14 \text{ cm}^{-1}$  and  $\Delta E_{\text{Right}} = 5572.46 \text{ cm}^{-1}$ . The  $\nu = 0$  energy level lies below the  $\nu = 1$  energy level by only  $177.32 \text{ cm}^{-1}$ , and their  $\langle R \rangle$  values lie at  $1.047$  Å for  $\nu = 0$  and  $2.353$  Å for  $\nu = 1$ , as given in Table 3. We can clearly assign the  $\nu = 0$  state to the left well (E state) and the  $\nu = 1$  state to the right well (F state). The  $\nu = 2$  level can be assigned to the right well since  $\langle R \rangle = 2.413$  Å. The  $\nu = 3$  and  $\nu = 4$  levels again lie close to each other with the splitting of only  $182.45 \text{ cm}^{-1}$ , and they are assigned to the left and the right wells, respectively. The  $\nu = 5$  level is assigned to the right well. The  $\nu = 6$  energy level is calculated to be  $E = -152027.49 \text{ cm}^{-1} = -0.692688 \text{ a.u.}$ , which is near the local maximum energy value of the  $E_1$  (EF)  $^1\Sigma_g$  potential curve,  $E = -0.690747 \text{ a.u.}$  at  $R = 3.0 \text{ a.u.}$ , and the  $\langle R \rangle$  value of the  $\nu = 6$  state is  $1.514$  Å. This implies that the  $\nu = 6$  state is delocalized over the two wells. The  $\nu = 7$  level is somewhat localized again in the right well since the  $\langle R \rangle$  values are about  $2.305$  Å. All of the vibrational states above  $\nu = 8$  are delocalized and they are mixed states of E and F states since their absolute energies are higher than the top of the hill. If the double wells are completely symmetric, then two vibrational states should always become degenerate. In the present case, since the E and F shapes are similar to each other, the states:  $\nu = 0$  and 1 and

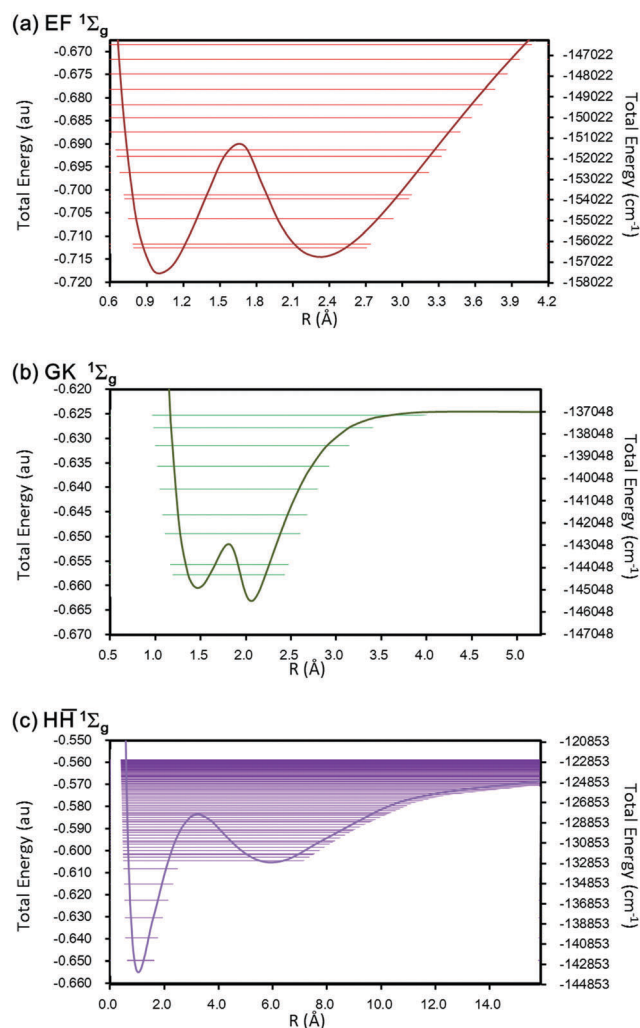


**Fig. 14** Vibrational energy levels (horizontal lines) associated with the double-well potential energy curves for the (a) EF, (b) GK, and (c) H $\bar{H}$  states of the  $^1\Sigma_g$  symmetry.

$\nu = 3$  and 4 nearly degenerate only with the energy gaps: 177.32 and 182.45  $\text{cm}^{-1}$ , respectively. Therefore, only with small thermal effects, the vibrational levels would shift between the left and the right by the tunneling process.

For the GK state, the energy barriers are quite small, *i.e.*  $\Delta E_{\text{Left}} = 1977.47 \text{ cm}^{-1}$  and  $\Delta E_{\text{Right}} = 2519.57 \text{ cm}^{-1}$ , compared with those of the EF and H $\bar{\text{H}}$ . The number of the vibrational states below the hill, therefore, was only 2. The lowest one:  $\nu = 0$  is assigned to the right well and the  $\nu = 1$  state is assigned to the left well with the energy gap: 456.76  $\text{cm}^{-1}$ . Thus, each well has one vibrational state.

For the H $\bar{\text{H}}$  state, the shape of the left well is sharp but that of the right side is very broad since it is on the ionic curve proportional to  $1/R$ . A lot of vibrational states belonging to the right well were obtained. From  $\nu = 0$  to 5, all their vibrational levels are assigned to the left well. The lowest vibrational state assigned to the right is  $\nu = 6$ . In the vibrational states of  $\nu = 0$  to 27, the number of states belonging to the right well is 17 and, in contrast, only 4 to the left. The energy intervals between the neighboring two vibrational states belonging to the right well were calculated around 800  $\text{cm}^{-1}$  (maximum) to 200  $\text{cm}^{-1}$  (minimum). The energy gaps between  $\nu = 14$  and 15 and  $\nu = 23$  and 24 were incidentally small: 98.1 and 84.6  $\text{cm}^{-1}$ , respectively. However, the coupling of these vibrational states would be small because the positions of the left and right minima:  $R = 1.050$  and 6.152 Å were apart and their energy barriers:  $\Delta E_{\text{Left}} = 15391.76 \text{ cm}^{-1}$  and  $\Delta E_{\text{Right}} = 5682.20 \text{ cm}^{-1}$  were also very different from each other.

Similar discussions can be accomplished for the vibrational levels for the other double-well PECs as seen in the ESI.† In the BO approximation, however, the vibrational analysis of a PEC having a complicated shape would highly depend on how to analyze the PEC, *i.e.* fitting function, the number of discrete points to fit the analytical curve, *etc.* Moreover, non-adiabatic effects become significant for these states. In such a case, we will need a non-BO treatment to obtain accurate vibrational states.<sup>11,12,46</sup>

## VI. Concluding remarks

We have systematically solved the Schrödinger equation of hydrogen molecules for the ground and excited states of the  $^1\Sigma_g$ ,  $^1\Sigma_u$ ,  $^3\Sigma_g$ , and  $^3\Sigma_u$  symmetries and obtained their accurate potential energy curves with the free complement variational method within the BO approximation. The calculated energies were very accurate, considered as essentially exact solutions, and guaranteed to be the upper bound to the exact energies due to the variational principle. We could describe the very small van der Waals minima ( $\sim 5 \text{ cm}^{-1}$  depth) in the excited states very accurately. All the PECs were calculated in a common comprehensive manner according to the FC theory: the energies and wave functions of the ground and excited states were obtained simultaneously from the same secular equations. It guarantees that the wave functions of different states are orthogonal and Hamiltonian orthogonal to each other as shown by eqn (2) and (3).

Therefore, even the complicated PECs that relate to the ionic contribution were also accurately described. To describe the dissociation limits accurately, it is better to introduce the ionic term and higher Rydberg functions corresponding to  $2p_z$ ,  $3p_z$ , *etc.* orbitals of hydrogen atoms from the initial function. Since it may cause computational difficulty for integrations near dissociations, we did not introduce them to the present case. However, in the upcoming paper<sup>40</sup> by the FC-LSE method where no integration problem occurs, these functions are introduced as the initial function and the PECs will be well described up to dissociation.

Based on the essentially-exact PECs by the FC theory, we also numerically solved the vibrational Schrödinger equations comprehensively for all the electronic ground and excited states calculated in this paper. In particular, we discussed the vibrational states on the double-well PECs of EF, GK, and H $\bar{\text{H}}$  states of  $^1\Sigma_g$ . The double-well potential of the H $\bar{\text{H}}$  state originates from the mixing of the ionic contributions. The present data and analysis should be valuable for experimental studies and useful as accurate reference data, in particular for future investigations in astronomical studies.

However, the non-adiabatic effects would often become significant especially for higher electronic excited states, and vibrational analysis often depends on computational conditions especially for the PECs having complicated or broad shapes. For these states, the non-BO approach is interesting<sup>11,12,46</sup> and will be performed in the near future.

## Conflicts of interest

There are no conflicts to declare.

## Acknowledgements

This work was supported by the JSPS KAKENHI Grant Numbers 17KT0103, 17H06233, 26810014, 16K17864, and 16H02257. The computations were performed using the Research Center for Computational Science (IMS), Okazaki, Japan, and partially provided by the RIKEN Advanced Institute for Computational Science, Kobe, Japan, through the HPCI System Research Project (Project ID: hp140140). The authors sincerely thank the gracious support provided by these computer centers. The authors thank Dr T. Miyahara for valuable comments.

## References

- 1 H. Nakatsuji, *J. Chem. Phys.*, 2000, **113**, 2949.
- 2 H. Nakatsuji, *Phys. Rev. Lett.*, 2004, **93**, 030403.
- 3 H. Nakatsuji, *Phys. Rev. A: At., Mol., Opt. Phys.*, 2005, **72**, 062110.
- 4 H. Nakatsuji, H. Nakashima, Y. Kurokawa and A. Ishikawa, *Phys. Rev. Lett.*, 2007, **99**, 240402.
- 5 H. Nakatsuji, *Acc. Chem. Res.*, 2012, **45**, 1480.
- 6 H. Nakashima and H. Nakatsuji, *J. Chem. Phys.*, 2007, **127**, 224104.
- 7 Y. I. Kurokawa, H. Nakashima and H. Nakatsuji, *Phys. Chem. Chem. Phys.*, 2008, **10**, 4486.

- 8 H. Nakashima and H. Nakatsuji, *Phys. Rev. Lett.*, 2008, **101**, 240406.
- 9 A. Ishikawa, H. Nakashima and H. Nakatsuji, *J. Chem. Phys.*, 2008, **128**, 124103.
- 10 A. Ishikawa, H. Nakashima and H. Nakatsuji, *Chem. Phys.*, 2012, **401**, 62.
- 11 Y. Hijikata, H. Nakashima and H. Nakatsuji, *J. Chem. Phys.*, 2009, **130**, 024102.
- 12 H. Nakashima, Y. Hijikata and H. Nakatsuji, *Astrophys. J.*, 2013, **770**, 144.
- 13 Y. Kurokawa, H. Nakashima and H. Nakatsuji, *Phys. Rev. A: At., Mol., Opt. Phys.*, 2005, **72**, 062502.
- 14 A. Bande, H. Nakashima and H. Nakatsuji, *Chem. Phys. Lett.*, 2010, **496**, 347.
- 15 H. Nakatsuji and H. Nakashima, *TSUBAME e-Science J.*, 2014, **11**(8), 24.
- 16 H. Nakatsuji and H. Nakashima, *J. Chem. Phys.*, 2015, **142**, 084117.
- 17 H. Nakatsuji and H. Nakashima, *J. Chem. Phys.*, 2015, **142**, 194101.
- 18 H. M. James and A. S. Coolidge, *J. Chem. Phys.*, 1933, **1**, 825; H. M. James and A. S. Coolidge, *J. Chem. Phys.*, 1935, **3**, 129.
- 19 J. S. Sims and S. A. Hagstrom, *J. Chem. Phys.*, 2006, **124**, 094101.
- 20 W. Kolos and L. Wolniewicz, *J. Chem. Phys.*, 1965, **43**, 2429.
- 21 W. Kolos and L. Wolniewicz, *Chem. Phys. Lett.*, 1974, **24**, 457.
- 22 L. Wolniewicz and K. Dressler, *J. Chem. Phys.*, 1985, **82**, 3292.
- 23 L. Wolniewicz, *J. Chem. Phys.*, 1993, **99**, 1851.
- 24 W. Kolos, *J. Chem. Phys.*, 1994, **101**, 1330.
- 25 L. Wolniewicz and K. Dressler, *J. Chem. Phys.*, 1994, **100**, 444.
- 26 T. Orlikowski, G. Staszewska and L. Wolniewicz, *Mol. Phys.*, 1999, **96**, 1445.
- 27 G. Staszewska and L. Wolniewicz, *J. Mol. Spectrosc.*, 1999, **198**, 416.
- 28 G. Staszewska and L. Wolniewicz, *J. Mol. Spectrosc.*, 2002, **212**, 208.
- 29 See references in J. Rychlewski and J. Komasa, in *Explicitly Correlated Wave Functions in Chemistry and Physics—Theory and Applications*, ed. J. Rychlewski, Kluwer Academic, Dordrecht, 2003, pp. 91–147.
- 30 W. Cencek, J. Komasa and J. Rychlewski, *Chem. Phys. Lett.*, 1995, **246**, 417.
- 31 M. Stanke, D. Kdziera, S. Bubin, M. Molski and L. Adamowicz, *J. Chem. Phys.*, 2008, **128**, 114313.
- 32 G. Corongiu and E. Clementi, *J. Chem. Phys.*, 2009, **131**, 034301.
- 33 E. Clementi and G. Corongiu, *Int. J. Quantum Chem.*, 2008, **108**, 1758.
- 34 K. Pachucki, *Phys. Rev. A: At., Mol., Opt. Phys.*, 2010, **82**, 032509.
- 35 K. Pachucki, *Phys. Rev. A: At., Mol., Opt. Phys.*, 2013, **88**, 022507.
- 36 J. W. Liu and S. Hagstrom, *J. Phys. B: At., Mol. Opt. Phys.*, 1994, **27**, L729.
- 37 K. Pachucki and J. Komasa, *Phys. Rev. A: At., Mol., Opt. Phys.*, 2011, **83**, 042510.
- 38 T. E. Sharp, *At. Data*, 1971, **2**, 119.
- 39 A. Pardo, *Spectrochim. Acta, Part A*, 1994, **50**, 941.
- 40 H. Nakashima and H. Nakatsuji, *J. Chem. Phys.*, submitted.
- 41 Computer code *MAPLE*, Waterloo Maple Inc., Waterloo, Ontario, Canada; see <http://www.maplesoft.com>.
- 42 About the GMP library, see <http://www.cs.nyu.edu/exact/core/gmp>.
- 43 R. J. Le Roy, Level 8.0: A Computer Program for Solving the Radial Schrödinger Equation for Bound and Quasibound Levels, University of Waterloo Chemical Physics Research Report CP-663, 2007; see <http://leroy.uwaterloo.ca/programs/>.
- 44 E. R. Davidson, *J. Chem. Phys.*, 1960, **33**, 1577; E. R. Davidson, *J. Chem. Phys.*, 1961, **35**, 1189.
- 45 D. Bailly, E. J. Salumbides, M. Vervloet and W. Ubachs, *Mol. Phys.*, 2010, **108**, 827.
- 46 H. Nakashima and H. Nakatsuji, *J. Chem. Phys.*, 2013, **139**, 074105.